Nuclear Instruments and Methods in Physics Research A 349 (1994) 412–417
North-Holland

NUCLEAR INSTRUMENTS & METHODS IN PHYSICS RESEARCH
Section A

Further test and development of the micro-gap chamber

F. Angelini [a], R. Bellazzini [a,*], A. Brez [a], M.M. Massai [a], R. Raffo [a], G. Spandre [a], M. Spezziga [a], M. Bozzo [b]

[a] *INFN-Pisa and University of Pisa, Pisa, Italy*
[b] *INFN-Genova and University of Genova, Genova, Italy*

Received 5 April 1994

Results from a beam test of the micro-gap chamber with minimum ionizing particles are reported. The dependence of the spatial resolution on the incidence angle of the beam with respect to the detector plane has been studied. Laboratory tests on new amplification structures, designed to increase gain and stability and to reduce the detector capacitance, are also shown. A maximum gas gain of 6000 and a specific capacitance of 0.5 pF/cm have been obtained. An optimised layout of the MGC's structure to avoid edge effects is discussed.

1. Introduction

Since its appearance [1] on the stage of ultraminiaturized radiation detectors, the micro-gap chamber has proven to be a really innovative concept, well suited for the tracking systems of future high energy physics experiments as well as for many other applications. Peculiar to its structure is the separation of only a few microns between the anode and the positive ion collecting cathode, and a pitch which can range from 1 mm down to 50 μm. Due to the large number of field lines ending on the very close back-cathode and to the steep voltage gradient, the process of avalanche charge collection is very fast. 90% of the total charge is delivered to the preamplifier in 10 ns. In the same time an almost equal amount of charge is induced on the back-cathode strips. Furthermore, the high electric field which extends over a very small region is not affected by the anode pitch. This permits easy design of a detector with variable pitch (the "keystones" structure) as required in the forward discs of the LHC tracking systems [2,3]. Another interesting characteristic of the device is its intrinsic two-dimensional nature. The near cathode can in fact be suitably structured allowing reconstruction of a coordinate not necessarily orthogonal to the anode strips. Other structures, i.e. radial, stereo or pads, can be chosen as well. All the above aspects make the micro-gap chamber a further improvement of the microstrip gas detector as concerns speed, spatial resolution and flexibility.

This paper reports on the detector test with minimum ionizing particles and on laboratory studies on new amplification structures designed to further increase gas gain and stability and to reduce the strip capacitance.

* Corresponding author. Tel. +39 50 880 271, Fax +39 50 880 317.

2. Test beam: experimental set-up and results

The test has been performed at the CERN SPS with a 300 GeV/c π^- beam.

The micro-gap chamber (Fig. 1) was part of a telescope [4], made of two standard MSGCs of the type already used in the NA12 experiment [5] and one micro-gap chamber, installed inside the RD5 superconducting magnet.

A silicon microstrip telescope was used as an external position reference system. In the trigger a small 2×2 cm^2 counter defined a beam spot of the size of the microstrip chambers. The MGC was mounted on a rotating frame which allowed inclination of the chamber with respect to the beam line (Fig. 2).

The fast readout chain used in this test was the same already used with a similar set-up in the NA12 experiment [5]. The delta current response of the shaping amplifier (Laben 5185) was adjusted to have a 10 ns rise-time and a 50 ns width (FWHM). The anode signals were recorded individually by means of LeCroy 2282 ADC.

A simple cluster algorithm allowed the determination of the charge cluster produced by the particle, whose coordinate was then computed with the center of gravity method. The difference between the measured and the expected coordinate, as derived from the silicon telescope, has been computed. The spatial resolution (analog) was then estimated from the rms width of the distribution of the track residuals quadratically subtracting the contribution due to the silicon detectors. With a simpler algorithm,

0168-9002/94/$07.00
SSDI 0168-9002(94)00670-3

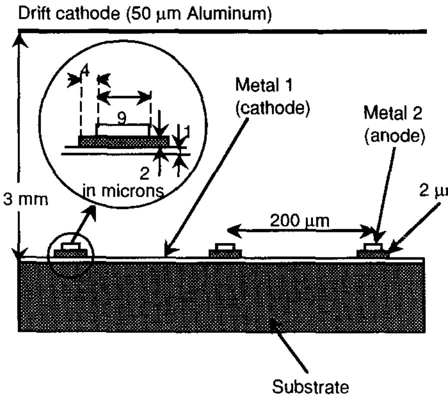

Fig. 1. A schematic cross section of the detector used in the test beam.

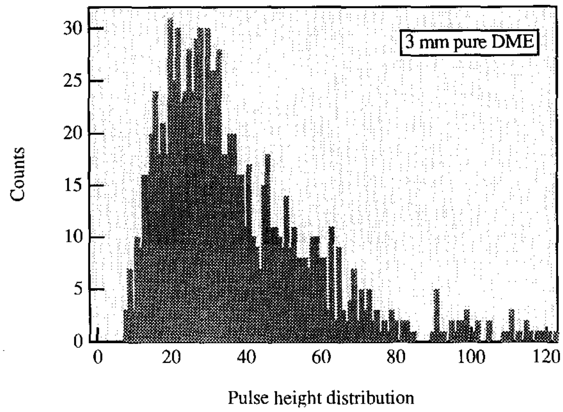

Fig. 3. A typical Landau distribution at a gas gain ~ 1000.

which assigns the same weight to all the strips in the cluster, the digital resolution has been evaluated too.

During the test we have used an MGC with a 3 mm gas gap, 9 μm anode width 200 μm pitch and 2 μm inter-metal oxide layer, of the type already described in a previous paper [1]. The gas filling was pure DME which has a high cluster density (~ 60 cluster/cm) and a small diffusion coefficient. The operating drift field was 1 kV/mm. At such high field the drift velocity of pure DME is > 5 cm/μs [6]. The efficiency, obtained in conditions of gas gain ~ 1000, was 99% (cathode voltage = −450 V). In Fig. 3 a pulse height distribution with the typical Landau shape is shown. For normal particle incidence we have measured an analog spatial resolution of 37 μm (rms) and a digital one of 57 μm (rms). To study the resolution as a function of the track angle, the chamber was rotated around an axis parallel to the anode strips. Fig. 4 shows the dependence on the particle incidence angle of both the analog and digital resolution. The analog resolution is better at small angles while at angles greater than 15° the digital algorithm gives better resolution. This effect can be explained by the fact that, while the digital resolution is affected only by the fluctuations of the number of strips over threshold, the analog resolution is affected also by the large fluctuations of the avalanche charge collected by each strip.

3. New structures and laboratory tests

Although the device with 2 μm oxide thickness has proven to perform well and to be reasonably robust and reliable, nevertheless further improvements in gain and stability can be obtained with suitable changes in the design of the amplification structure. Fig. 5 shows the new micro-gap structures we have already built and tested (a–d), and one structure (e) that we are going to implement. For all these structures a thicker silicon oxide layer,

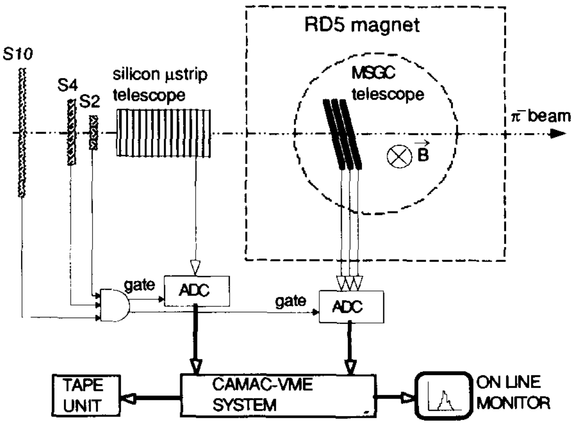

Fig. 2. A schematic view of the test beam set-up.

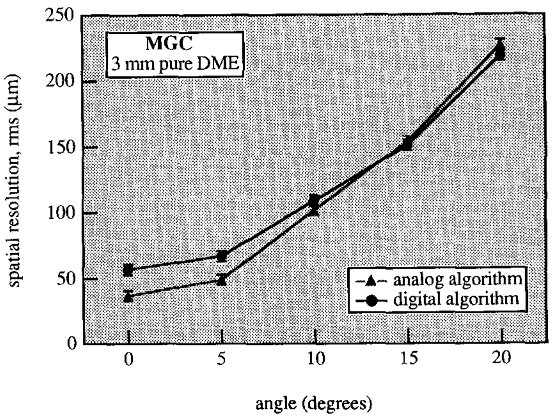

Fig. 4. The spatial resolution (analog and digital) as a function of the particle incidence angle.

3.5 or 5 μm instead of the previous 2 μm, has been deposited on metal 1. This allows an increase of the voltage applied to the cathode strips, and consequently increased gain, while maintaining safe conditions for the detector. Furthermore, the increase of the oxide thickness implies a decrease of the strip capacitance, thus improving the signal to noise ratio. Further reductions of the capacitance (see Table 1) are obtained by removing the metal 1 under the oxide layer everywhere except in last 1 or 2 μm on both sides of the layer (Fig. 5b and 5e) and/or by reducing the oxide width exactly to the size of the anode strip (Fig. 5c–5e). This has been obtained by using the so-called "self-aligned" technology, commonly used by the CMOS microelectronics industry. In this technology the anode pattern itself is used as a mask for the plasma etching of the intermetal oxide, thus guaranteeing a perfect, built-in, alignment of the anode strip with the oxide strip. With this last processing technique the number of masks needed for the detector construction is reduced to the minimum, i.e. one for the 1-D device and two for the 2-D device. Fig. 6 shows the electric field map obtained for a MGC with a 5 μm thick oxide built using the "self-alignment" technology and, comparatively, for the structure of Fig. 1 having a 2 μm oxide layer. The value of the electric field reported in Fig. 6 refers to the center of the strip.

Table 1
Total anode specific capacitance (pF/cm) for the various MGC structures (h_0 = oxide thickness, w = anode width)

	h_0 (μm)	$w = 5$ μm	$w = 9$ μm
a)	3.5	0.97	1.4
a)	5	0.77	1.1
b)	3.5	0.76	0.91
b)	5	0.67	0.81
c)	5	0.57	0.87
d)	5	0.47	0.60
e)	5	0.55	0.76

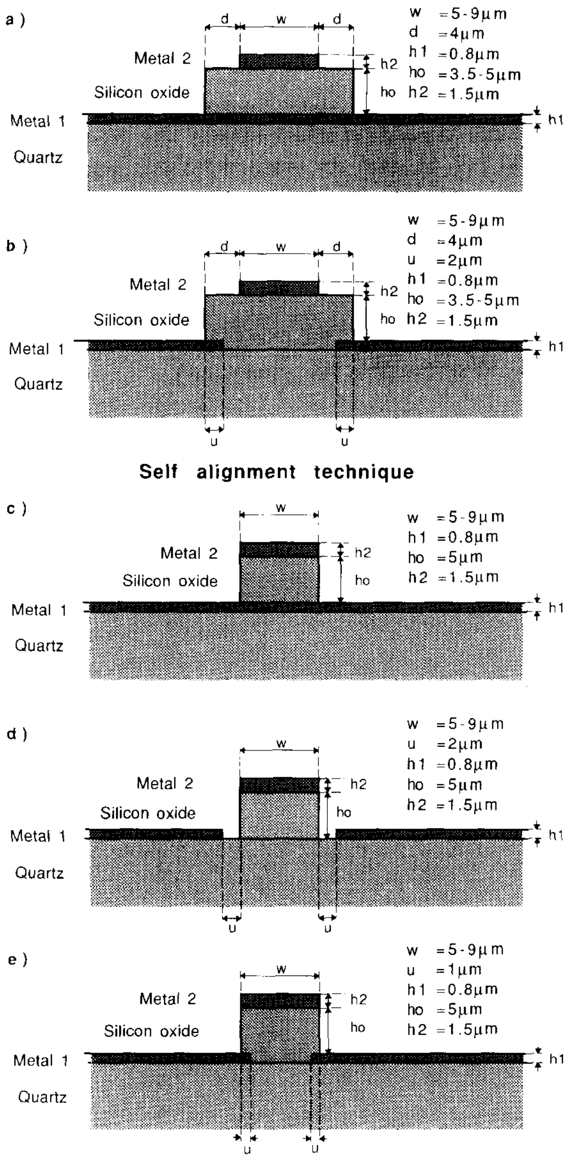

Fig. 5. The new micro-gap structures.

To study the dependence of the gain on the cathode voltage a laboratory test with X-ray sources has been carried out for each structure. A photo of the signal from the OR of three anod strips for the case of Fig. 5b is shown in Fig. 7 when working with 5.4 keV chromium X-rays.

An increase of gain with respect to the structures with 2 μm oxide thickness has been observed for all the detectors under test, except for the MGC of Fig. 5d. In this case the cathode edges, left exposed in the gas and not buried under

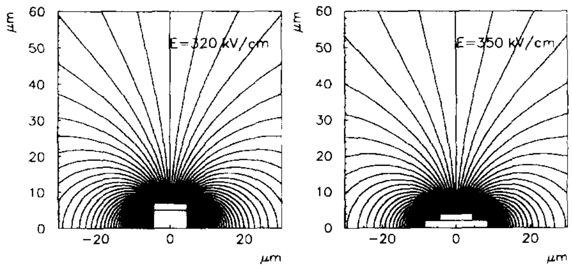

Fig. 6. The electric field map obtained for a typical configuration in the "self-alignment" technology (left) and for the MGC of Fig. 1 (right).

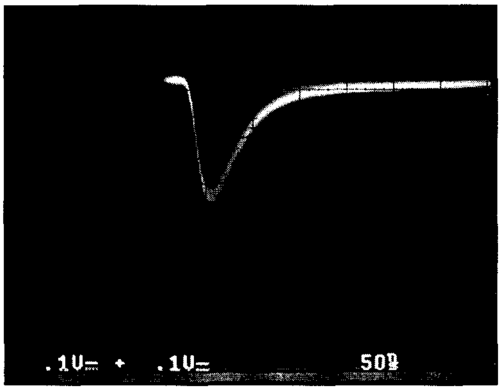

Fig. 7. The signal from the OR of three anode strips for the case b) of Fig. 5.

the oxide, let earlier sparking to develop. Fig. 8 shows the pulse height dependence with the cathode voltage for the tested structures. A maximum gain of ~ 6000 has been obtained for the structure of Fig. 5a.

4. Optimization of the detector layout

The weak point for all kinds of microstrip gas detectors is the terminal part of both the anode and cathode strips. Because of edge effects the electric field is reinforced in these points and, if no special precautions are taken, sparking starts to develop here. The maximum achievable gain is therefore limited by this effect. We have tried to tackle this problem by designing the electrode ends in such a way that the maximum of the field strength is confined within the normal straight section of the amplifying cell [7]. Fig. 9a shows a photograph of one end of a 5 μm wide anode strip. The photo refers to a MGC of the type shown in Fig. 5b. Fig. 9b shows the opposite side (the readsout side) in which the anode–cathode separation has been progressively increased before arriving at the cathode strip end. Further safety factors have been provided by: a) removing the intermetal oxide only in the straight section of the cell but avoiding removal where the strips end; and b) adding on top of the anode–cathode structure, at the detector border, a 25 μm thick passivation layer (300 μm wide). The layer is made of curable polyimide, a material with a very high dielectric strength (~ 300 kV/mm). With

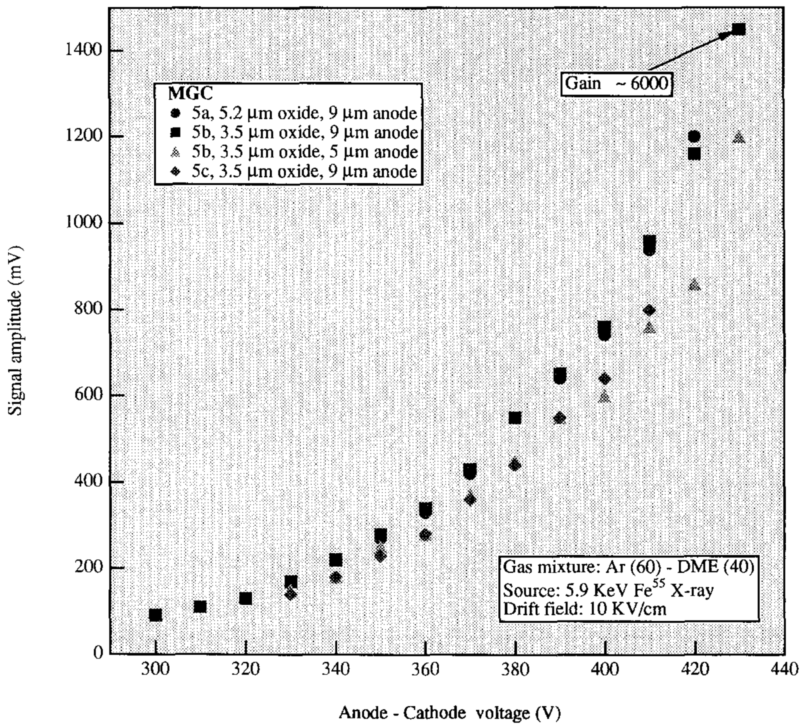

Fig. 8. The pulse height dependence on cathode voltage for the new structures.

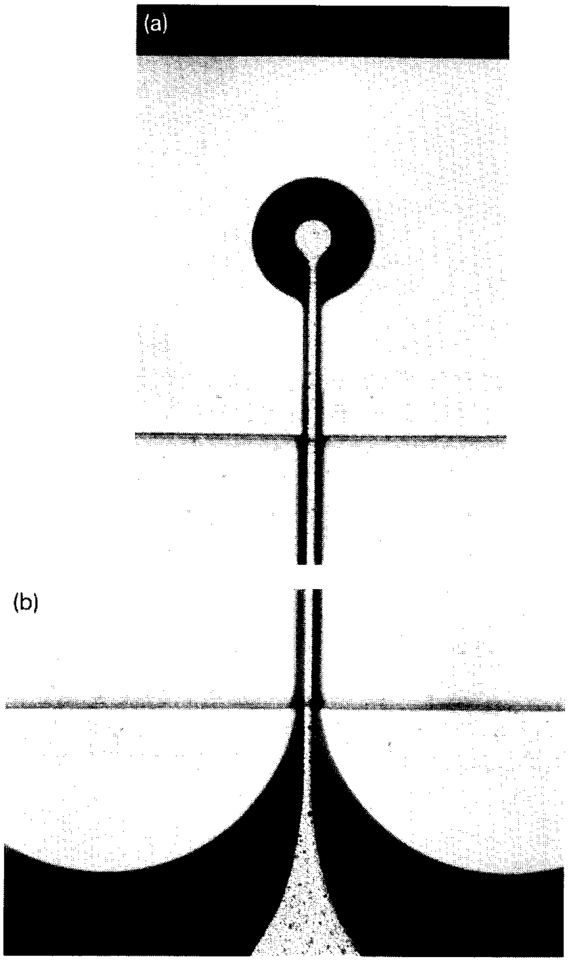

Fig. 9. A photograph of a detail of the optimized layout of the edges of anode (a) and cathode (b) strips.

these precautions sparking has not been observed at these points.

5. Conclusions

Even if still evolving, the micro-gap chamber has already proven to be a strong reality. Because no cathode edge is left exposed, the detector is very safe and more robust and spark free than the conventional MSGC for the same signal amplitude. A gas gain of 6000 can be achieved with structures having very low specific capacitance (~ 0.5 pF/cm). Full efficiency and good spatial resolution (< 40 μm, rms) can be obtained even when operating with very thin gas layers. Our efforts are now directed toward the development of large area (10×10 cm^2 or more), 2-D devices. If this development is successful, the MGC could probably supersede the MSGC in many applications, including those extremely demanding ones coming from the high energy physics experiments.

Acknowledgements

We want to express our gratitude to all the RD5 team for their hospitality and help. We thank G. Decarolis, M. Favati, C. Magazzu' and S. Tolaini of INFN-Pisa and A. Morelli of INFN-Genova for their enthusiastic technical support.

References

[1] F. Angelini et al., Nucl. Instr. and Meth. A 335 (1993) 69.
[2] CMS Collaboration, Letter of Intent, CERN/LHCC 92–4.
[3] ATLAS Collaboration, Letter of Intent, CERN/LHCC 92–4.
[4] F. Angelini et al., INFN PI/AE 93/17, accepted for publication on Nucl. Instr. and Meth.
[5] F. Angelini et al., Nucl. Instr. and Meth. A 315 (1992) 21.
[6] M. Geijsberts et al., Nucl. Instr. and Meth. A 313 (1992) 377.
[7] A. Oed et al., Nucl. Instr. and Meth. A 310 (1991) 95.